

Supporting information for

## Rapid Flow in Multilayer Microfluidic Paper-Based Analytical Devices

Robert B. Channon,<sup>a†</sup> Michael P. Nguyen,<sup>a†</sup> Alexis G. Scorzelli,<sup>b</sup> Elijah M. Henry,<sup>a</sup> John Volckens,<sup>c</sup> David S. Dandy,<sup>d</sup> and Charles S. Henry<sup>a\*</sup>

a. Department of Chemistry, Colorado State University, Fort Collins, Colorado 80523, United States

b. Department of Chemistry and Physics, Monmouth University, West Long Branch, New Jersey 07764, United States

c. Department of Mechanical Engineering, Colorado State University, Fort Collins, Colorado 80523, United States

d. Department of Chemical and Biological Engineering, Colorado State University, Fort Collins, Colorado 80523, United States

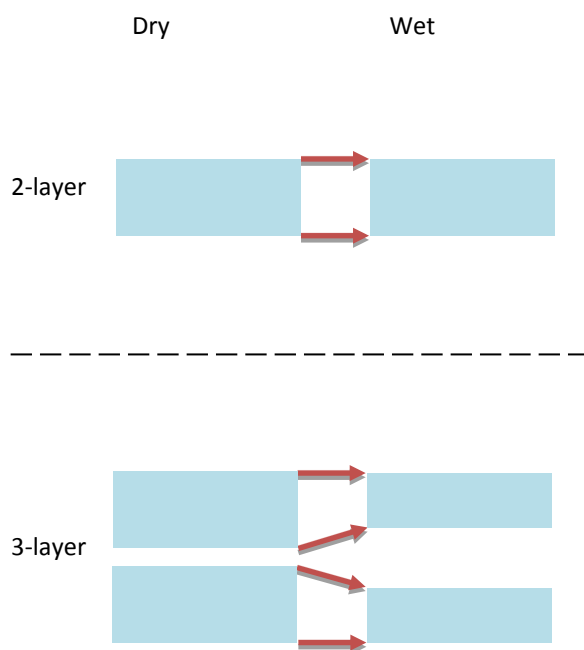


**Figure S1.** Side on illustration of swelling in 2- and 3-layer  $\mu$ PADs, where blue is fluid, red is paper and grey is the tape sealing. Note that as the paper wets, the channel height in the 2-layer device stays the same as the paper pushes on the tape, but the channel height is reduced in the 3-layer device due to swelling of the middle paper layer (red arrows).

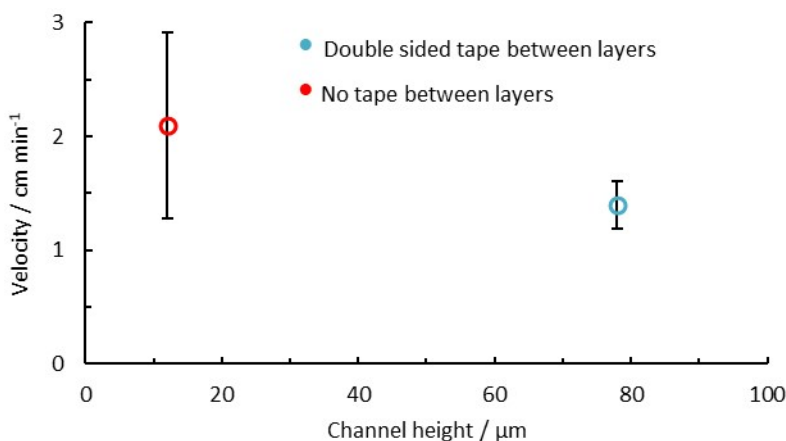


**Figure S2.** Effect of confining channel height with or without double sided sticky tape on the velocity for multilayer  $\mu$ PADs, vertical orientation, ( $n = 5$ ) flow taken up to 5.55 cm. The channel height for the untapped device is an estimate based on previous multilayer  $\mu$ PAD publications.<sup>1,2</sup>

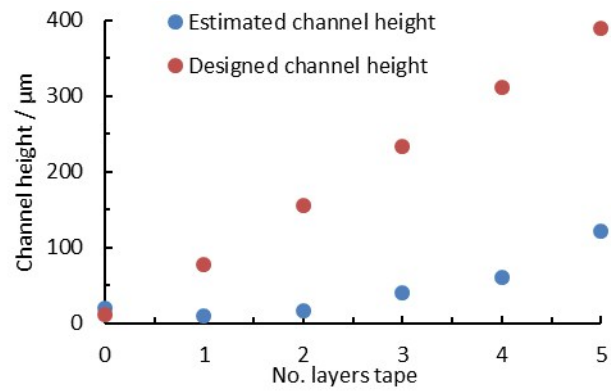


**Figure S3.** Estimated channel height from theoretical models based on the observed device velocities and actual channel height based on design of the multilayer  $\mu\text{PADs}$ , for horizontally orientated devices.

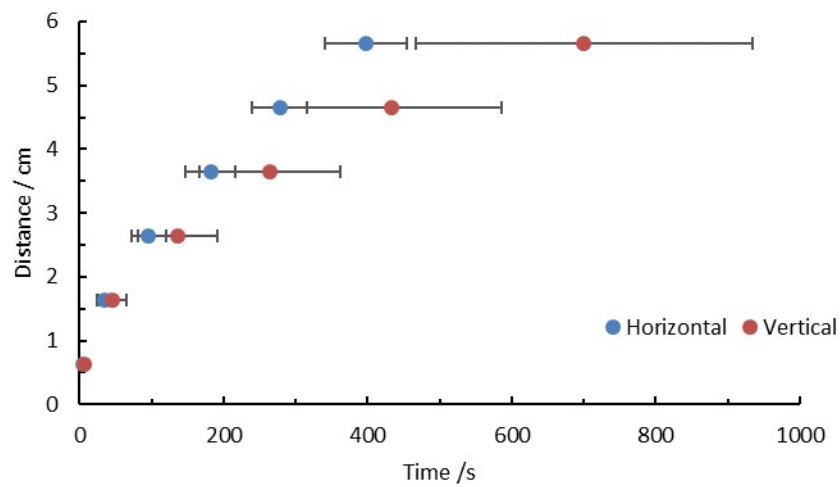


**Figure S4.** Length traversed down straight channel 1-layer of paper  $\mu\text{PADs}$  with horizontal and vertical orientation ( $n = 5$ ).

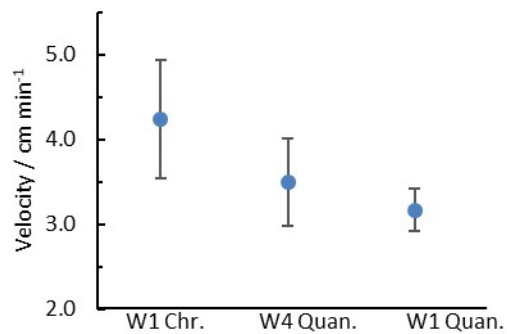


**Figure S5.** Effect of paper type on flow rate using vertical  $\mu$ PADs with 3 layers of tape between the two paper layers. Velocity is calculated for flow up to 5.55 cm ( $n = 5$ ).

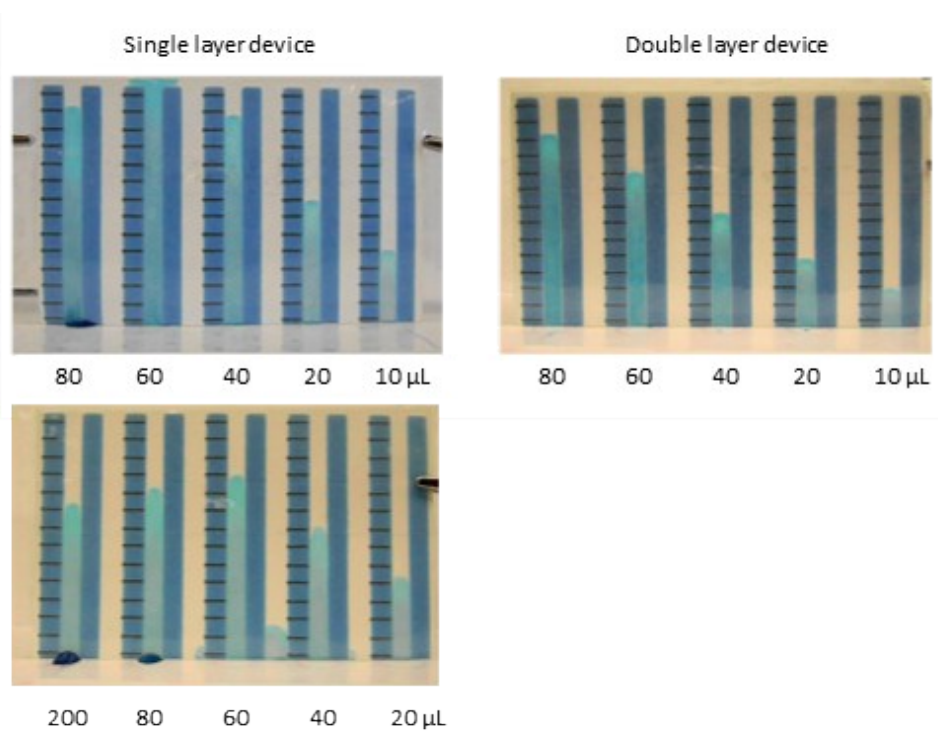


**Figure S6.** Photographs of volume dependent fluid transport in single vs double layer devices, as described in Figure 5 of the main paper. Top: comparison of single and double paper layer devices with 10, 20, 40, 60, and 80  $\mu$ L dye. Bottom: snapshot of single layer device during flow, showing slower flow rates at inlet volumes above 60  $\mu$ L.

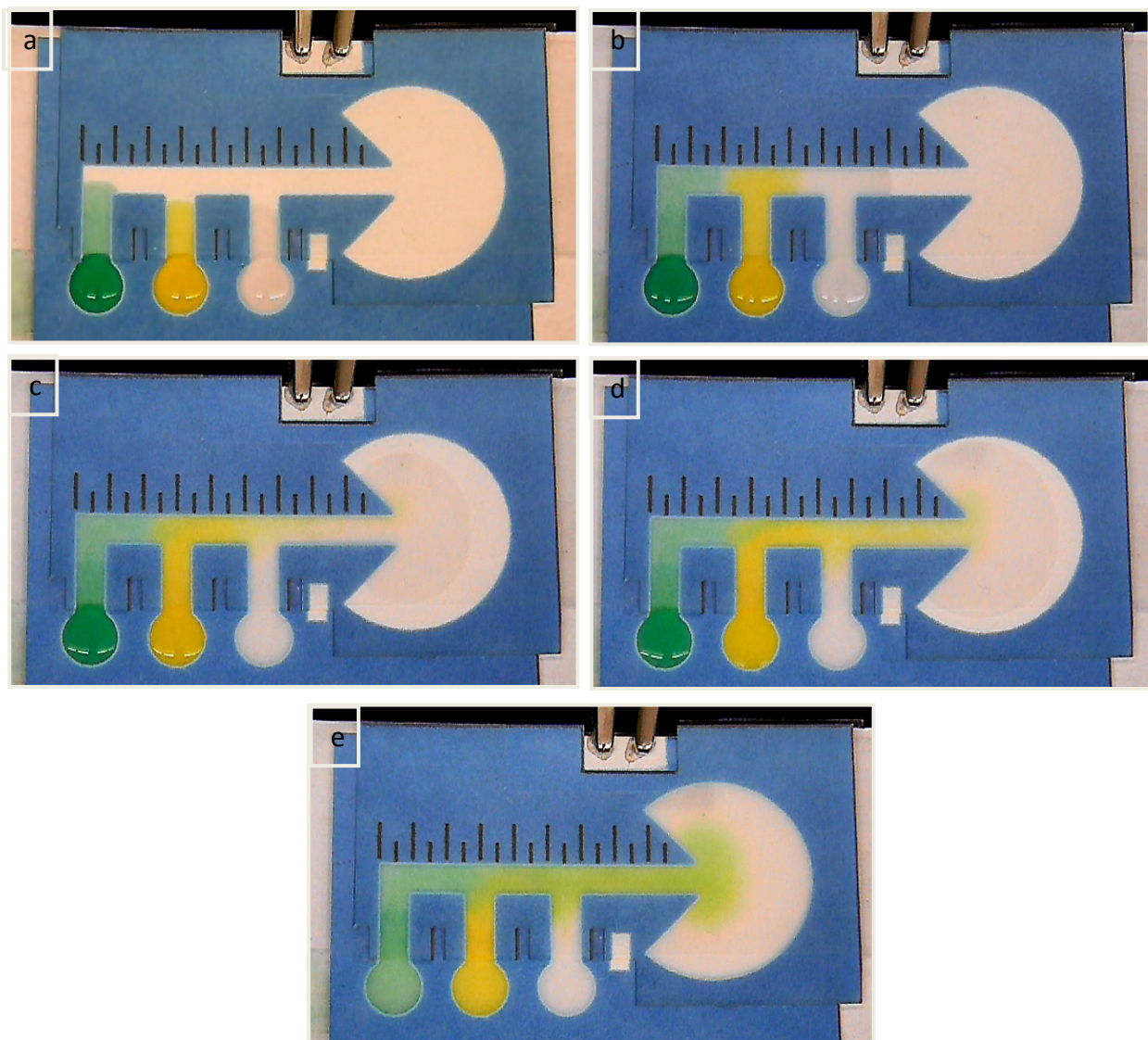


**Figure S7.** Images of a multilayered 3DPN device using 3 layers of tape between the layers, at different stages of sequential injection (Figure 6 if main paper, blue line). The 80  $\mu\text{L}$  injections from right to left are as follows:  $\text{KNO}_3$ , 1 mM  $\text{FcTMA}^+$  with 0.1 M  $\text{KNO}_3$  spiked with a yellow dye, and finally 0.1 M  $\text{KNO}_3$  spiked with a green dye. The snapshots represent a) addition of sample to wells and wicking up the inlet legs, b)  $\text{KNO}_3$  reaching the electrodes, c)  $\text{FcTMA}^+$

reaching the electrodes, d) The maximum current signal from the FcTMA<sup>+</sup> injection, e) the final (wash) KNO<sub>3</sub> injection washes the FcTMA<sup>+</sup> past the electrode and the flow ceases as the fan is filled and the sample wells are depleted.

## **REREFENCES**

1. J. A. Adkins, E. Noviana and C. S. Henry, *Anal. Chem.*, 2016, **88**, 10639-10647.
2. C. K. Camplisson, K. M. Schilling, W. L. Pedrotti, H. A. Stone and A. W. Martinez, *Lab Chip*, 2015, **15**, 4461-4466.